ELSEVIER

Thermochimica Acta 362 (2000) 59–70

thermochimica acta

www.elsevier.com/locate/tca

# Thermal and kinetic analysis of *ortho*-palladated complexes with pyridines

José Pérez[a,*], Gregorio Sánchez[a], Joaquín García[a], José Luis Serrano[b], Gregorio López[a]

[a]*Departamento de Química Inorgánica, Campus Universitario de Espinardo,Universidad de Murcia, 30071 Murcia, Spain*
[b]*Departamento de Ingeniería Minera y Cartográfica, Universidad Politécnica de Cartagena, 30203, Cartagena, Spain*

Received 6 March 2000; accepted 22 June 2000

**Abstract**

The complexes $[Pd(az)(\mu\text{-}X)]_2$ (az = 2(phenylazo)phenyl; X = Cl, Br, I) react with pyridines (L = pyridine, α-picoline and γ-picoline) to form the corresponding *ortho*-palladated derivatives [Pd(az)XL]. The compounds have been characterized by C, H and N analyses and spectroscopic methods (IR and $^1$H-NMR). TG, DTG and DSC studies of the complexes were carried out in dynamic nitrogen atmosphere. From DSC analyses the heats of decomposition were calculated. The kinetics of the first step of thermal decomposition were evaluated from TG data by isothermal and non-isothermal methods. The activation energies obtained are in the range 90–110 kJ mol$^{-1}$. The best fitting for isothermal data was observed for $R_n$ and $A_{1.5}$ kinetic models; for non-isothermal experiments the mechanisms that best fit the data are $R_n$ and $F_1$. 

*Keywords:* *Ortho*-palladated complexes; Thermal behaviour; Kinetic analysis

## 1. Introduction

The *ortho*-palladated compounds have been widely studied, since they are succesful starting materials for the synthesis of complexes of transition metals [1,2] and reactive intermediates in organic synthesis [3]. In 1965, Cope and Siekman [4] reported that tetrachloropalladate(II) ion reacts with azobenzene to give the dinuclear complex $[Pd(az)(\mu\text{-}Cl)]_2$. The most interesting features of this complex are its relatively high thermal stability (decomposes at 279–281°C) and the cleavage of its chloride bridges with phosphines and amines give the monomeric complexes [Pd(az)ClL] [4,5]. $^1$H-NMR data indicated that in acetone or dimethylsulphoxide solutions, some of these complexes (L = amines) dissociate to give the precursor $[Pd(az)(\mu\text{-}Cl)]_2$ and the free ligand L. Thermal studies on organometallic rhodium(III) [6,7], ruthenium(II) [8] and palladium(II) [9] derivatives have been previously reported. Thermogravimetric data of these complexes confirmed the high thermal stability of the chloro-bridged metal complexes.

Here, we describe the thermal behaviour of monomeric *ortho*-palladated complexes of the type [Pd(az)XL] (az = 2(phenylazo)phenyl, X = Cl, Br, I; L = pyridines) and the kinetic analysis for the first step of thermal decomposition, that was evaluated by isothermal and non-isothermal methods.

* Corresponding author. Tel.: +34-968-367454; fax: +34-968-364148.
*E-mail address*: jperez@fcu.um.es (J. Pérez).

0040-6031/00/$ – see front matter 
PII: S0040-6031(00)00590-6

## 2. Experimental

Pyridine, α-picoline, γ-picoline and azobenzene were obtained from commercial sources and all the solvents were dried by conventional methods before use.

### 2.1. Preparation of the complexes

The complex $[Pd(az)(\mu\text{-}Cl)]_2$ was prepared according to previously published methods [10]. The corresponding bromo- and iodo-bridged derivatives were obtained by metathetical reactions with lithium bromide and sodium iodide, respectively.

The complexes [Pd(az)XL] (X = Cl, L = py, α-picoline, γ-picoline; X = Br, I, L = py) were obtained by reaction of the dinuclear complexes $[Pd(az)(\mu\text{-}X)]_2$ (X = Cl, Br, I) with the corresponding pyridines in $CH_2Cl_2$ solution according to the following general method. An excess of neutral ligand (0.65 mmol) in dichloromethane (5 $cm^3$) was added to a solution of precursor $[Pd(az)(\mu\text{-}X)]_2$ (0.162 mmol) in dichloromethane (10 $cm^3$) and the mixture was boiled under reflux for 1 h. The resulting solution was concentrated under reduced pressure to half original volume. The addition of hexane caused the formation of yellow solids, which were filtered off, washed with diethyl ether and air dried.

### 2.2. Characterization

The C, H and N analyses were performed with a Carlo Erba microanalyser. Conductivities were measured with a Crison 525 conductimeter. IR spectra were recorded on a Perkin-Elmer 16F PC FT–IR spectrophotometer using Nujol mulls between polyethylene sheets. $^1$H-NMR data were recorded on a Bruker AC 200E instrument.

[Pd(az)Cl(py)] (**Ia**). Yield 81%. Analysis: found (%): C: 50.7; H: 3.6; N: 10.4; calcd. : C: 50.9; H: 3.3; N: 10.5. Non-conductor in acetone. IR ($cm^{-1}$) (Nujol): 1572, 1552, 766, 698 [2(phenylazo)phenyl]; 1602 (py); 324 (ν-PdCl). $^1$H-NMR (δ) [solvent $(CD_3)_2SO$; reference $SiMe_4$]: 8.6 (br, 2H), 8.0 (d, 1H), 7.9 (m, 1H), 7.6 (m, 2H), 7.3 (m, 8H).

[Pd(az)Cl(α-picoline)] (**Ib**). Yield 77%. Analysis: found (%): C: 52.1; H: 3.6; N: 9.8; calcd.: C: 51.9; H: 3.9; N: 10.1. Non-conductor in acetone. IR ($cm^{-1}$) (Nujol): 1574, 1552, 766, 694 [2(phenylazo)phenyl]; 1606 (α-picoline); 326 (ν-PdCl). $^1$H-NMR (δ) [solvent $(CD_3)_2SO$; reference $SiMe_4$]: 8.7 (br, 2H), 8.0 (d, 1H), 7.6 (br, 2H), 7.4 (m, 8H), 2.7 (br, 3H).

[Pd(az)Cl(γ-picoline)] (**Ic**). Yield 75%. Analysis: found (%): C: 51.8; H: 3.7; N: 9.9; calcd.: C: 51.9; H: 3.9; N: 10.1. Non-conductor in acetone. IR ($cm^{-1}$) (Nujol): 1570, 1552, 764, 698 [2(phenylazo)phenyl]; 1616 (γ-picoline); 346 (ν-PdCl). $^1$H-NMR (δ) [solvent $(CD_3)_2SO$; reference $SiMe_4$]: 8.5 (br, 2H), 8.0 (d, 1H), 7.7 (br, 2H), 7.5 (m, 3H), 7.3 (m, 5H), 2.4 (br, 3H).

[Pd(az)Br(py)] (**II**). Yield 84%. Analysis: found (%): C: 45.5; H: 2.9; N: 9.3; calcd.: C: 45.8; H: 2.9; N: 9.4. Non-conductor in acetone. IR ($cm^{-1}$) (Nujol): 1574, 1550, 770, 698 [2(phenylazo)phenyl]; 1602 (py). $^1$H-NMR (δ) [solvent $(CD_3)_2SO$; reference $SiMe_4$]: 8.6 (br, 2H), 8.0 (d, 1H), 7.9 (m, 1H), 7.4 (m, 10H).

[Pd(az)I(py)] (**III**). Yield 71%. Analysis: found (%): C: 41.1; H: 2.7; N: 8.3; calcd.: C: 41.4; H: 2.7; N: 8.5. Non-conductor in acetone. IR ($cm^{-1}$) (Nujol): 1574, 1550, 758, 692 [2(phenylazo)phenyl]; 1600 (py). $^1$H-NMR (δ) [solvent $(CD_3)_2SO$; reference $SiMe_4$]: 8.5 (br, 2H), 8.0 (d, 1H), 7.7 (m, 1H), 7.3 (m, 10H).

### 2.3. Thermal analysis

Thermoanalytical data were obtained from TG, DTG and DSC curves. TG and DTG curves were recorded on a Mettler TA-3000 system provided with a Mettler TG-50 thermobalance and DSC curves were recorded on a DSC-7 Perkin-Elmer instrument. The atmospheres used in different experiments were pure nitrogen flow (50 $cm^3$ $min^{-1}$). The sample mass range was of 4–7 mg.

## 3. Results and discussion

### 3.1. Thermal stability

The TG and DSC data of the complexes are summarized in Table 1. All the complexes decompose on heating to give the binuclear complexes $[Pd(az)(\mu\text{-}X)]_2$, according to Eq. (1).

$$[Pd(az)XL(s)] \rightarrow \frac{1}{2}[Pd(az)(\mu\text{-}X)]_2(s) + L(g) \qquad (1)$$

Table 1
TG and DTG data for the neutral palladium(II) complexes[a]

| Complex | Step | Temperature range (°C) | $DTG_{max}$ (°C) | Weight loss (%) found (calcd.) | Assignment | Enthalpy change (kJ $mol^{-1}$) |
|---|---|---|---|---|---|---|
| [Pd(az)Cl(py)] | 1 | 80.5–148.5 | 142 | 19.3 (19.7) | Py | 33.6 |
| | 2 | 271.5–300.5 | 288 | 23.7 | | |
| | 3 | 300.5–436.5 | 406 | 27.2 | | |
| | Residue | >600 | – | 28.3 (26.4) | Pd + C | |
| [Pd(az)Cl(α-pic)] | 1 | 75.5–141 | 133.5 | 21.8 (22.4) | α-pic | 30.5 |
| | 2 | 272–334 | 289.5 | 26.3 | | |
| | 3 | 334–487 | 467.0 | 25.0 | | |
| | Residue | >600 | – | 26.5 (25.5) | Pd + C | |
| [Pd(az)Cl(γ-pic)] | 1 | 118.5–181.5 | 174.5 | 22.4 (22.4) | γ-pic | 54.2 |
| | 2 | 275–300 | 289.5 | 22.3 | | |
| | 3 | 339.5–470.5 | 449.5 | 27.3 | | |
| | Residue | >600 | – | 25.5 (25.5) | Pd + C | |
| [Pd(az)Br(py)] | 1 | 91.5–153.5 | 147.5 | 17.3 (17.7) | Py | 32.2 |
| | 2 | 277.5–324.5 | 292.0 | 30.8 | | |
| | 3 | 382–585 | 556.0 | 23.3 | | |
| | Residue | >600 | – | 26.2 (23.8) | Pd + C | |
| [Pd(az)I(py)] | 1 | 84.5–149.5 | 132.5 | 15.2 (16.0) | Py | 34.4 |
| | 2 | 235–544.5 | 247.0 | 52.3 | | |
| | Residue | >600 | – | 29.4 (21.5) | Pd + C | |

[a] Under dynamic nitrogen atmosphere; heating rate 6°C $min^{-1}$.

X = CL; L = pyridine, α-picoline, γ-picoline; X = Br, I; L = pyridine.

The halo-bridged binuclear complexes can be isolated in every case and identified by IR and $^1$H-NMR spectroscopy. The enthalpy changes for the first step were measured by integration of the endothermic peaks in the corresponding DSC curves (Table 1). The binuclear intermediates decompose slowly and irregularly between 235 and 544°C. On the bases of DTG peak temperatures, which correspond to the loss of the neutral ligands (heating rate: 6° $min^{-1}$), the thermal stability of the chloro-2(phenylazo)phenyl-palladium complexes can be placed in order as follows: [Pd(az)Cl(α-picoline)] < [Pd(az)Cl(py)] < [Pd(az)Cl(γ-picoline)], while the pyridine halocomplexes follow the order [Pd(az)I(py)] < [Pd(az)Cl(py)] < [Pd(az)Br(py)]. The sequence of thermal stability for the binuclear intermediate halo-complexes is $[Pd(az)(\mu\text{-I})]_2 < [Pd(az)(\mu\text{-Cl})]_2 < [Pd(az)(\mu\text{-Br})]_2$. The enthalpy changes for the release of the neutral ligands are practically constant for pyridine halo-complexes, while in the chloro-complexes the order followed is [Pd(az)Cl(α-pic)] < [Pd(az)Cl(py)] < [Pd(az)Cl(γ-pic)].

### 3.2. Kinetic analysis

#### 3.2.1. Isothermal analysis

The isothermal TG curves for the palladium complexes at different temperatures are shown in Figs. 1–5. The plots are approximately linear over an appreciable α range (e.g. $0.1 \leq \alpha \leq 0.5$), before becoming deceleratory.

The differential kinetic equation can be expressed as

$$\left(\frac{d\alpha}{dt}\right) = Ae^{-x}f(\alpha) \quad (2)$$

where $A$ is a pre-exponential factor for the Arrhenius type rate constant and $x$ the reduced apparent activation energy ($x = E_a/RT$). The function $f(\alpha)$ in Eq. (2) is an analytical expression describing the kinetic model of the studied thermal decomposition process (Table 2).

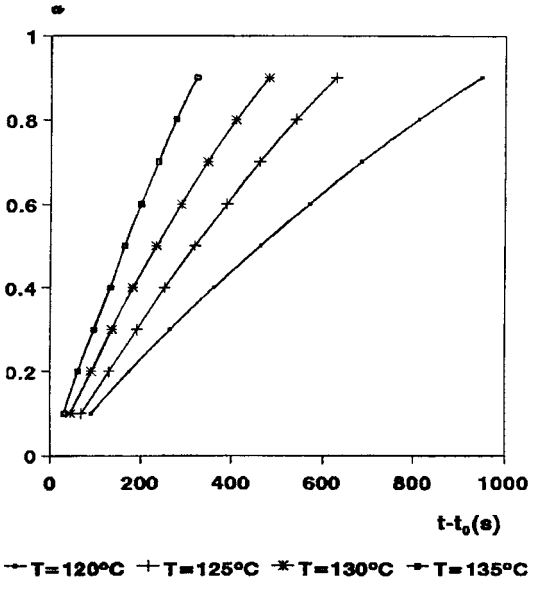


Fig. 1. Alpha vs. time plots for the first step of isothermal decomposition of [Pd(az)Cl(py)].

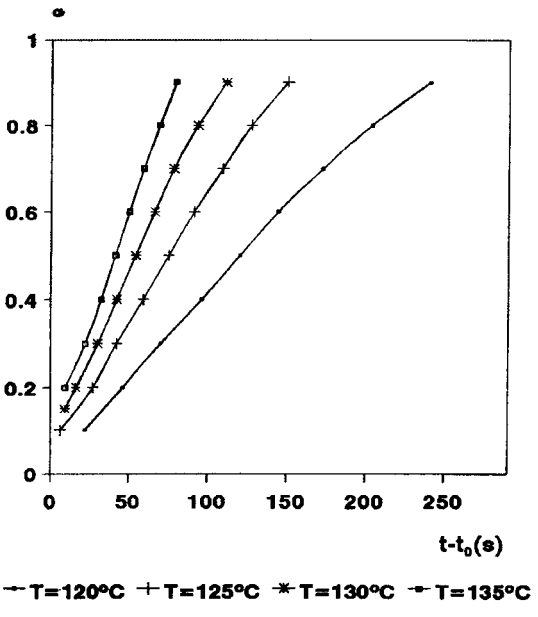


Fig. 2. Alpha vs. time plots for the first step of isothermal decomposition of [Pd(az)Cl(α-pic)].

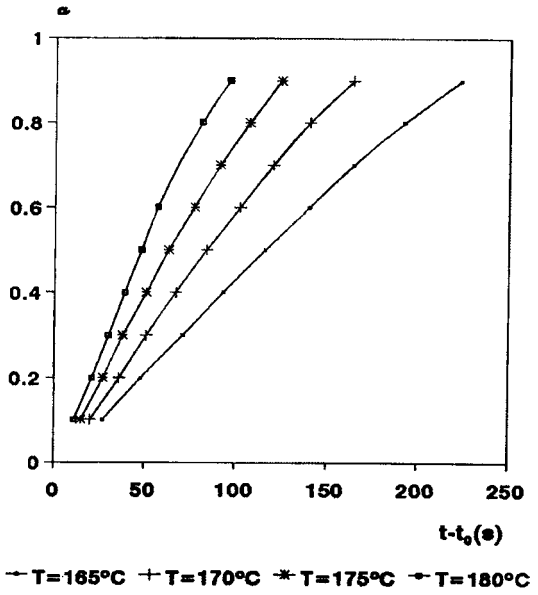


Fig. 3. Alpha vs. time plots for the first step of isothermal decomposition of [Pd(az)Cl(γ-pic)].

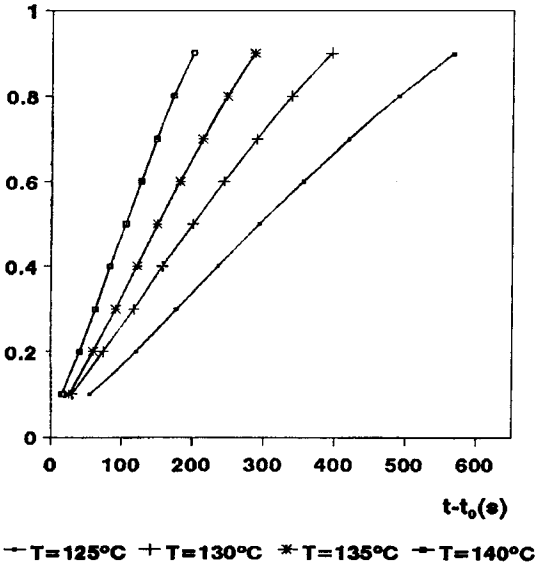


Fig. 4. Alpha vs. time plots for the first step of isothermal decomposition of [Pd(az)Br(py)].

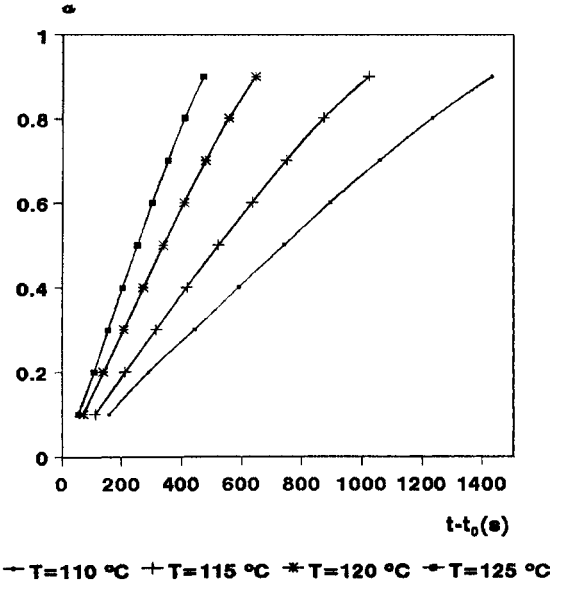


Fig. 5. Alpha vs. time plots for the first step of isothermal decomposition of [Pd(az)I(py)].

*3.2.1.1. Isoconversional method*. By integration of Eq. (2) in isothermal conditions the following equation is obtained:

$$g(\alpha) = A\mathrm{e}^{-x} \cdot t \tag{3}$$

The apparent activation energy of the decomposition process in isothermal conditions can be calculated by isoconversional method which follows from logarithmic form of Eq. (3):

$$\ln t = \ln\left[\frac{g(\alpha)}{A}\right] + \frac{E_a}{RT} \tag{4}$$

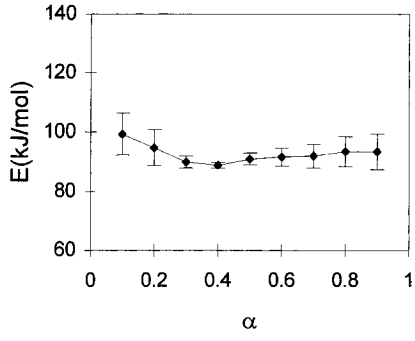


Fig. 6. Plot of apparent activation energy calculated from isothermal TG data by the isoconversional method as a function of α for [Pd(az)Cl(py)].

The slope of ln $t$ versus $1/T$ for the same value of α gives the value of apparent activation energy. This procedure can be repeated for various values of α. The plots of $E_a$ as a function of fractional conversion are shown in Figs. 6–10 within the certain error limits (specified by bars). The average values of apparent activation energy determined in the $0.2 < \alpha < 0.9$ range are $93 \pm 4$, $96 \pm 7$, $95 \pm 2$, $93 \pm 4$ and $92 \pm 5$ for the complexes **Ia**, **Ib**, **Ic**, **II** and **III**, respectively.

*3.2.1.2. Plots of the integrated rate functions, g(α), against time*. The linearity of the plots of the integrated rate functions, $g(\alpha)$, against time over the range $0.2 \leq \alpha \leq 0.9$ was assessed using the correlation coefficient ($r$). It was difficult to distinguish between applicability of the $A_{1.5}$, $A_2$ and $R_2$ models. Arrhenius plots constructed using $k$ values from the acceptable $g(\alpha)$ functions gave the apparent activation energies and the pre-exponential factors presented in Table 3. The

Table 2
Rate laws used to analyse kinetic data

| Mechanism | $f(\alpha)$ | $g(\alpha)$ |
|---|---|---|
| $D_1$ | $1/2\alpha$ | $\alpha^2$ |
| $D_2$ | $-1/\ln(1-\alpha)$ | $(1-\alpha)\ln(1-\alpha)+\alpha$ |
| $D_3$ | $3(1-\alpha)^{2/3}/\{2[1-(1-\alpha)^{1/3}]$ | $[1-(1-\alpha)^{1/3}]^2$ |
| $F_1$ | $1-\alpha$ | $-\ln(1-\alpha)$ |
| $F_2$ | $(1-\alpha)^2$ | $1/(1-\alpha)$ |
| $R_2$ | $2(1-\alpha)^{1/2}$ | $1-(1-\alpha)^{1/2}$ |
| $R_3$ | $3(1-\alpha)^{2/3}$ | $1-(1-\alpha)^{1/3}$ |
| $A_{1.5}$ | $3/2(1-\alpha)[-\ln(1-\alpha)]^{1/3}$ | $[-\ln(1-\alpha)]^{2/3}$ |
| $A_2$ | $2(1-\alpha)[-\ln(1-\alpha)]^{1/2}$ | $[-\ln(1-\alpha)]^{1/2}$ |
| $A_3$ | $3(1-\alpha)[-\ln(1-\alpha)]^{2/3}$ | $[-\ln(1-\alpha)]^{1/3}$ |

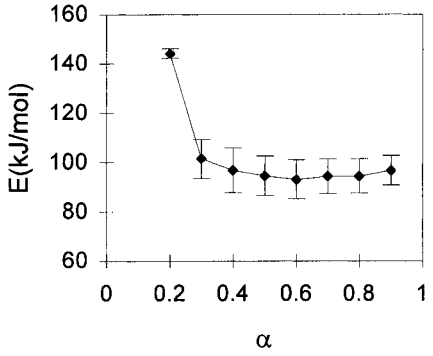


Fig. 7. Plot of apparent activation energy calculated from isothermal TG data by the isoconversional method as a function of α for [Pd(az)Cl(α-pic)].

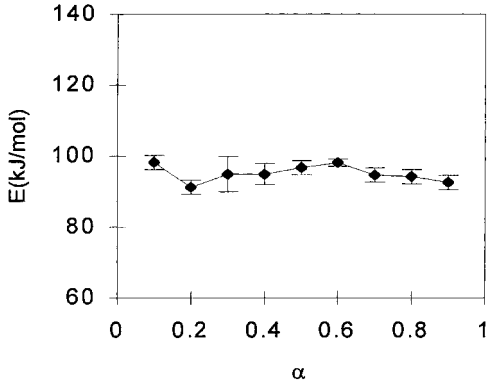


Fig. 8. Plot of apparent activation energy calculated from isothermal TG data by the isoconversional method as a function of α for [Pd(az)Cl(γ-pic)].

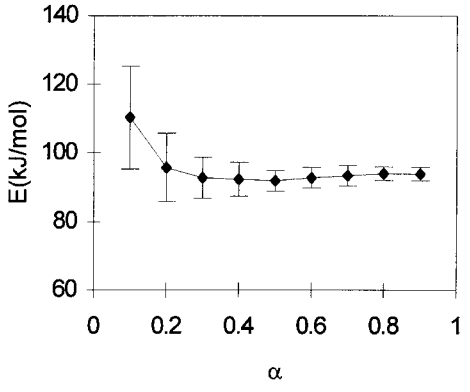


Fig. 9. Plot of apparent activation energy calculated from isothermal TG data by the isoconversional method as a function of α for [Pd(az)Br(py)].

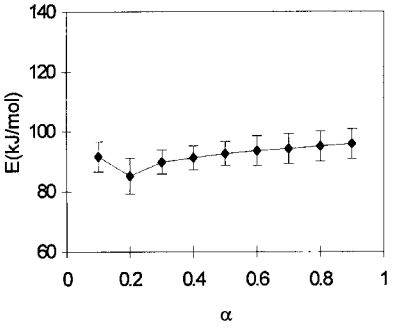


Fig. 10. Plot of apparent activation energy calculated from isothermal TG data by the isoconversional method as a function of α for [Pd(az)I(py)].

values of $E_a$ are almost independent of the physical model proposed and similar to that found by the isoconversional method.

*3.2.1.3. Reduced-time plots*. For a isokinetic process, if the times required to attain a set value of α (e.g. $\alpha = 0.5$) at several different (isothermal) temperatures are determined ($t_{0.5}$), then plots of α against reduced time ($t_{red} = t/t_{0.5}$) can be prepared [11]. This method consists in comparing the experimental data (in the form of reduced time) with the well-known calculated data for the models in Table 2. As can be seen from Figs. 11–15, the equation $A_{1.5}$ is the one that best fits the experimental results.

Table 3
Arrhenius parameters for the isothermal reactions

| Models | $E_a$ (kJ mol$^{-1}$) | $r$ | ln(A s$^{-1}$) |
|---|---|---|---|
| $A_{1.5}$ | | | |
| [Pd(az)Cl(py)] | 94 ± 6 | 0.9949 | 22.5 ± 1.9 |
| [Pd(az)Cl(α-pic)] | 94 ± 6 | 0.9963 | 23.8 ± 1.7 |
| [Pd(az)Cl(γ-pic)] | 94 ± 2 | 0.9997 | 20.8 ± 0.5 |
| [Pd(az)Br(py)] | 93 ± 1 | 0.9998 | 22.2 ± 0.3 |
| [Pd(az)I(py)] | 97 ± 5 | 0.9976 | 23.8 ± 1.5 |
| $A_2$ | | | |
| [Pd(az)Cl(py)] | 93 ± 6 | 0.9978 | 21.9 ± 1.9 |
| [Pd(az)Cl(α-pic)] | 94 ± 6 | 0.9964 | 23.6 ± 1.7 |
| [Pd(az)Cl(γ-pic)] | 93 ± 2 | 0.9997 | 20.5 ± 0.5 |
| [Pd(az)Br(py)] | 93 ± 1 | 0.9999 | 22.0 ± 0.3 |
| [Pd(az)I(py)] | 97 ± 5 | 0.9976 | 23.6 ± 1.5 |
| $R_2$ | | | |
| [Pd(az)Cl(py)] | 93 ± 6 | 0.9954 | 21.2 ± 1.9 |
| [Pd(az)Cl(α-pic)] | 94 ± 6 | 0.9964 | 23.1 ± 1.7 |
| [Pd(az)Cl(γ-pic)] | 93 ± 2 | 0.9997 | 20.0 ± 0.5 |
| [Pd(az)Br(py)] | 93 ± 1 | 0.9999 | 21.4 ± 0.3 |
| [Pd(az)I(py)] | 97 ± 5 | 0.9976 | 23.0 ± 1.5 |

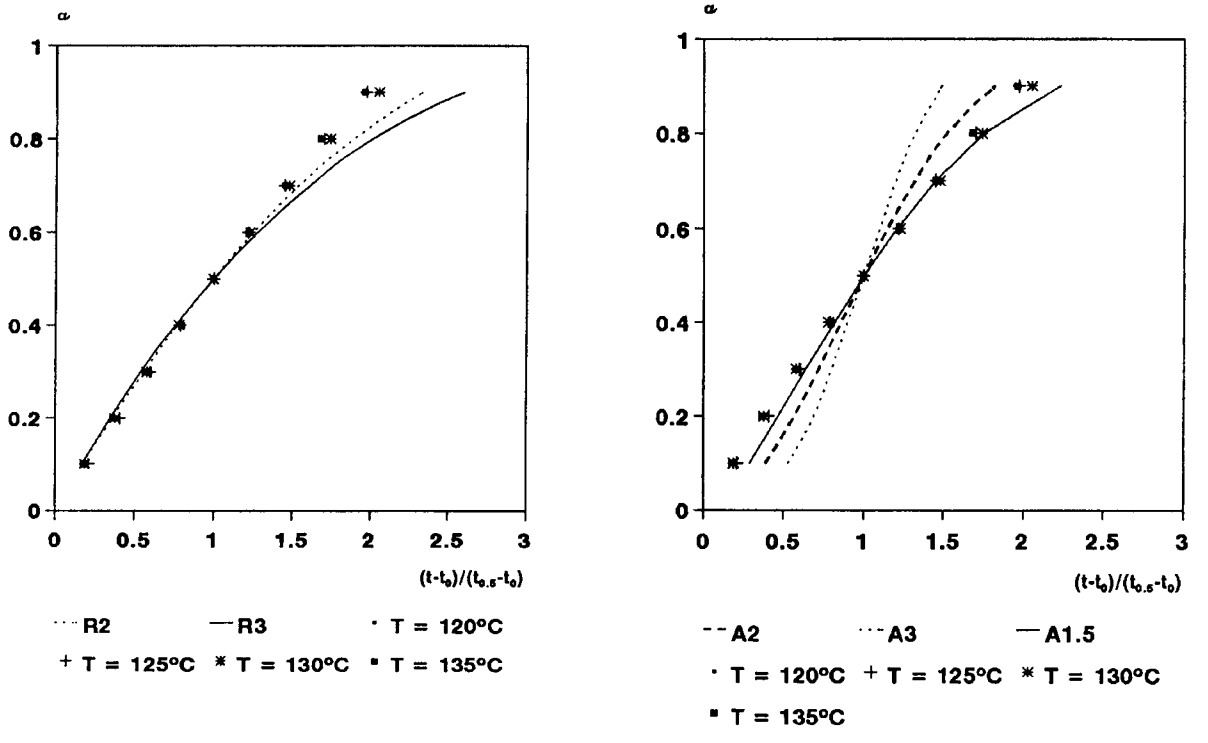


Fig. 11. Plots of reduced-time for [Pd(az)Cl(py)].

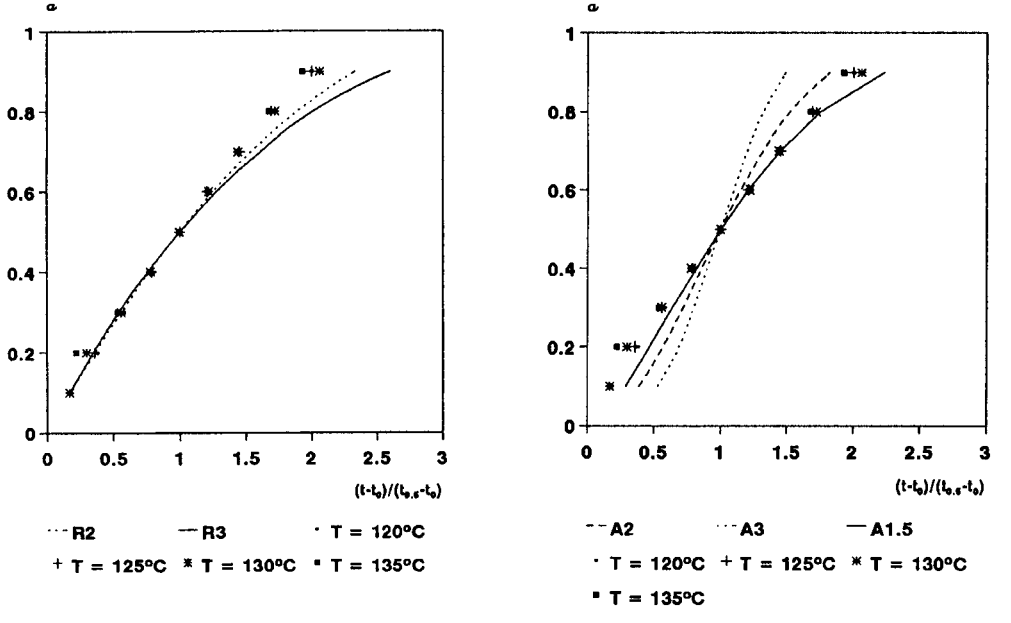


Fig. 12. Plots of reduced-time for [Pd(az)Cl(α-pic)].

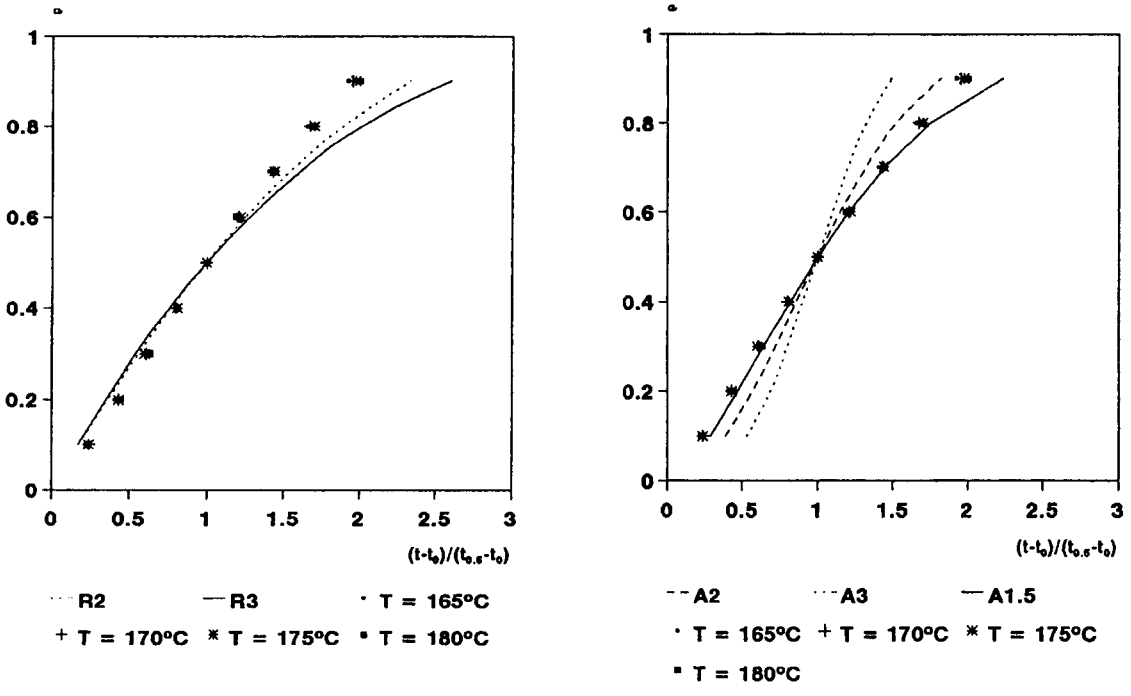


Fig. 13. Plots of reduced-time for [Pd(az)Cl(γ-pic)].

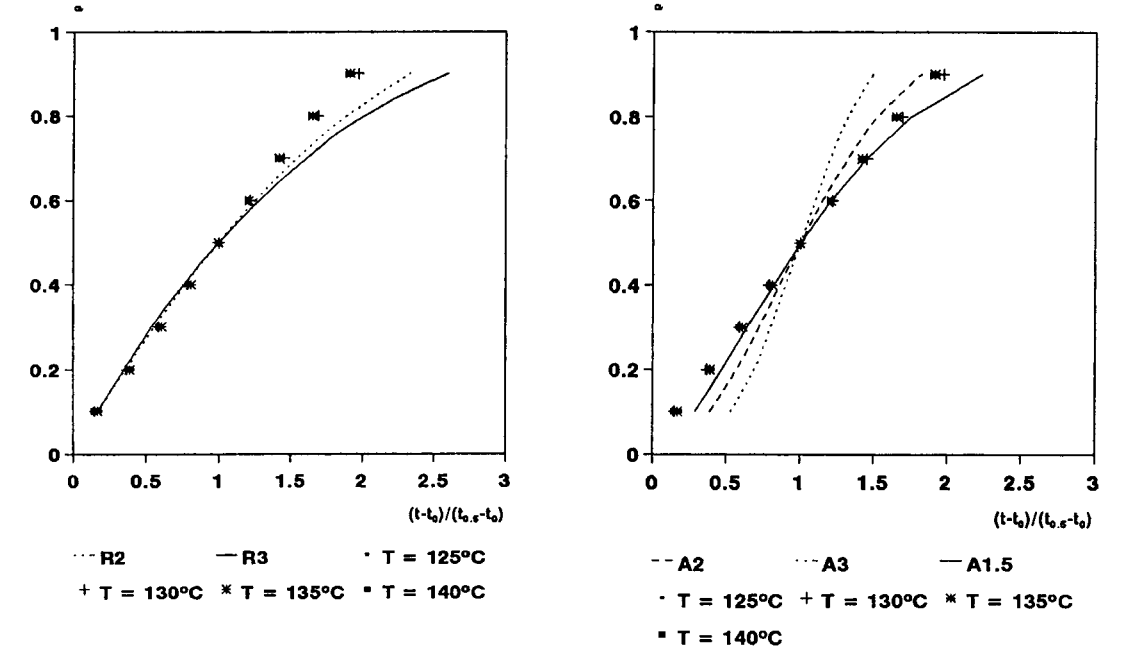


Fig. 14. Plots of reduced-time for [Pd(az)Br(py)].

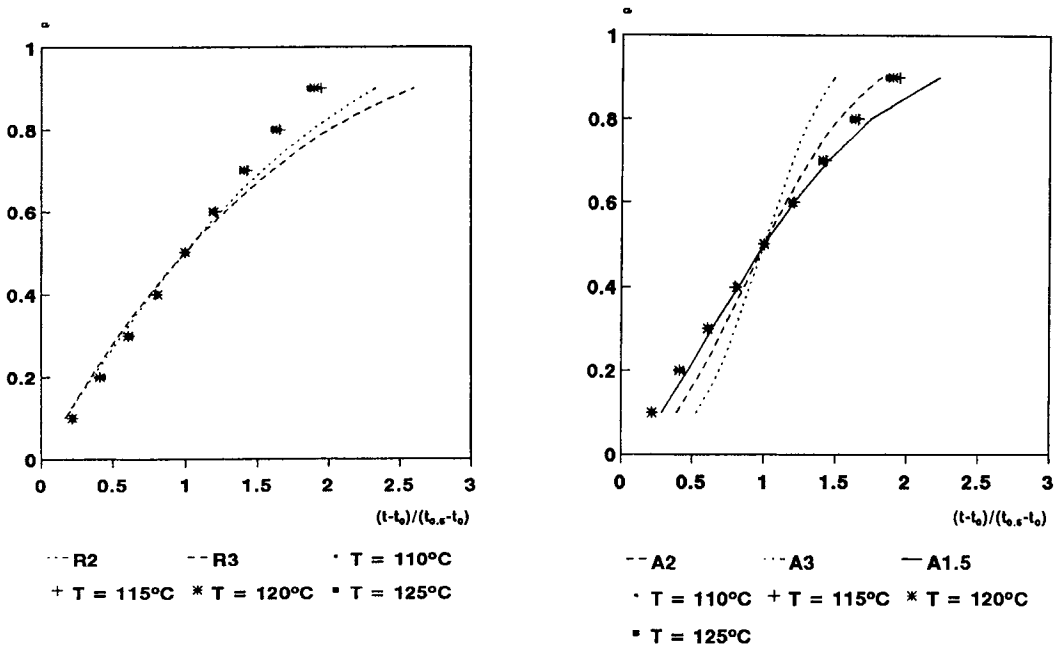


Fig. 15. Plots of reduced-time for [Pd(az)I(py)].

*3.2.2. Non-isothermal analysis*

Figs. 16–20 show the series of TG curves at 2, 3, 4 and 6° $min^{-1}$ for the first step of the studied processes. An isoconversional method [12] and the Coats–Redfern method [13] were used to study the non-isothermal kinetic.

*3.2.2.1. Isoconversional method.* By integration of Eq. (2) in non-isothermal conditions the following equation is obtained:

$$g(\alpha) = \left(\frac{AE}{\beta R}\right) p(x) \tag{5}$$

Doyle [14] has suggested that $\log p(x)$ can be approximated by the function:

$$\log p(x) = -2.315 - 0.4567x \tag{6}$$

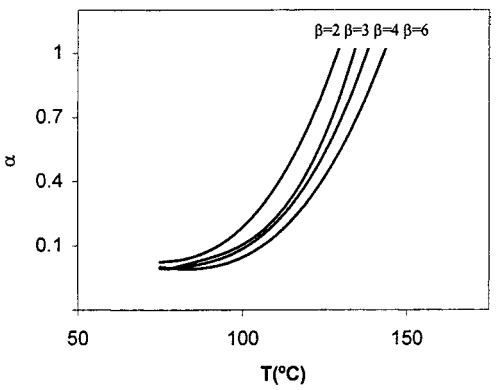


Fig. 16. TG curves for the first step of non-isothermal decomposition of [Pd(az)Cl(py)].

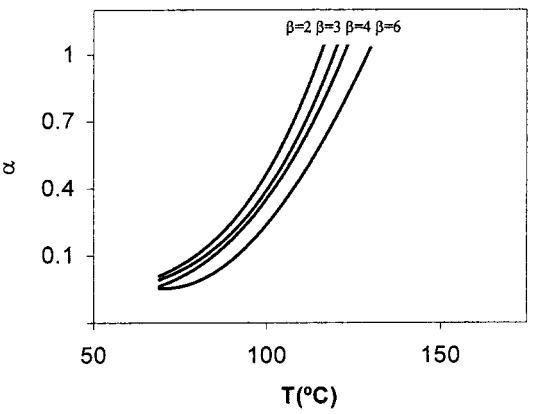


Fig. 17. TG curves for the first step of non-isothermal decomposition of [Pd(az)Cl(α-pic)].

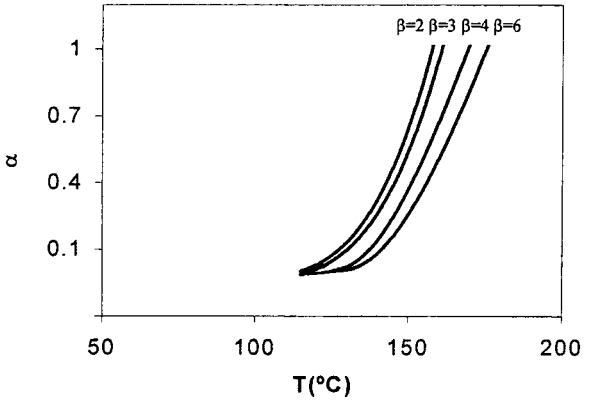


Fig. 18. TG curves for the first step of non-isothermal decomposition of [Pd(az)Cl(γ-pic)].

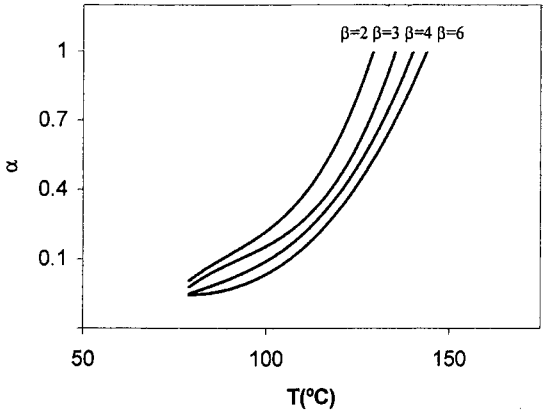


Fig. 19. TG curves for the first step of non-isothermal decomposition of [Pd(az)Br(py)].

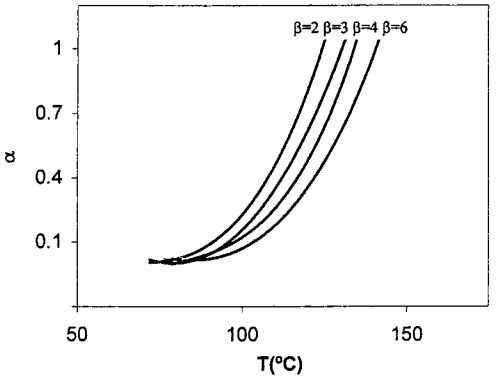


Fig. 20. TG curves for the first step of non-isothermal decomposition of [Pd(az)I(py)].

By combining Eqs. (5) and (6) we obtain the expression:

$$\log g(\alpha) = \log\left(\frac{AE}{\beta R}\right) - 2.315 - \frac{0.456E}{RT} \quad (7)$$

For a number of experiments with different heating rates, $\beta$, we can write for the same extent of reaction $\alpha$:

$$-\log \beta = \frac{0.4567E}{RT} + \text{constant} \quad (8)$$

The plot of $\log \beta$ versus $1/T$ for a given value of $\alpha$ must give the activation energy $E_a$. This procedure was suggested by Ozawa [12] and Flynn [15] independently.

The isoconversional lines obtained in plotting $\log \beta$ versus the reciprocal of the temperature (Eq. (8)) at the same degree of conversion, are all parallel straight lines yielding the same activation energy and are shown in Figs. 21–25.

The value of energy is constant in the $0.1 < \alpha < 0.9$ range for the complex with X = Cl and L = py (Fig. 21), being the mean value in that interval $101 \pm 9$ kJ mol$^{-1}$. For the complexes with X = Br, I, the energy is invariant with $\alpha$ in the $0.2 < \alpha < 0.9$ range with a mean value of $101 \pm 10$ and $88 \pm 3$ kJ mol$^{-1}$ as can be seen in Figs. 24 and 25. Regarding the chlorocomplexes with L = α-picoline and γ-picoline, the values of energy are similar in the $0.3 < \alpha < 0.9$ and $0.4 < \alpha < 0.9$ ranges, the mean

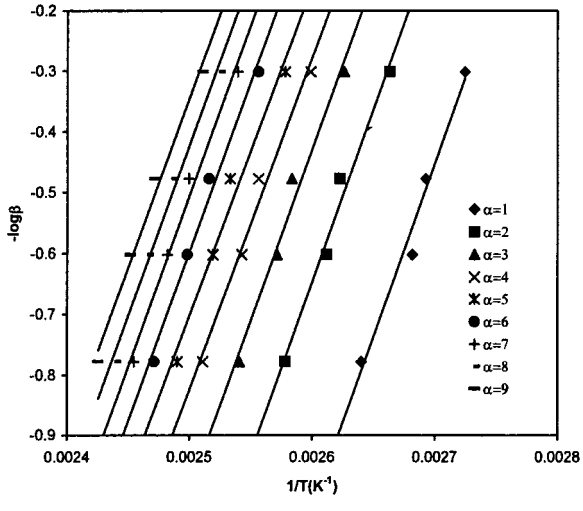


Fig. 21. Isoconversional plots for the non-isothermal decomposition of [Pd(az)Cl(py)].

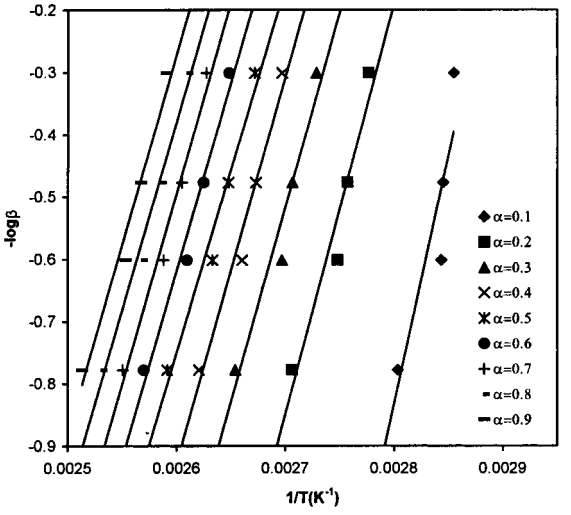


Fig. 22. Isoconversional plots for the non-isothermal decomposition of [Pd(az)Cl(α-pic)].

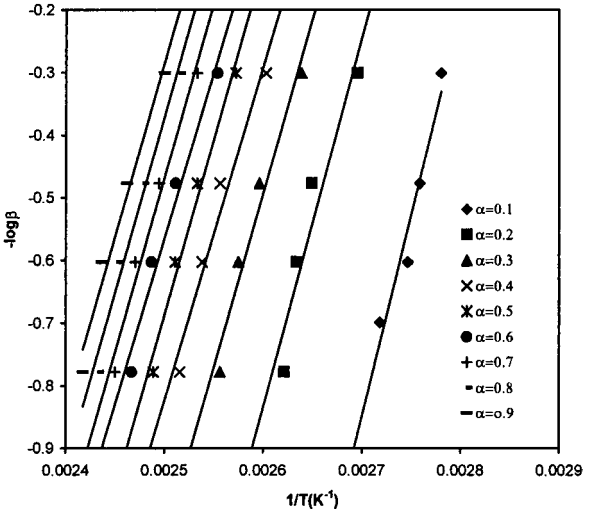


Fig. 24. Isoconversional plots for the non-isothermal decomposition of [Pd(az)Br(py)].

values are $111 \pm 12$ kJ mol$^{-1}$ for L = α-picoline and $102 \pm 13$ kJ mol$^{-1}$ when L = γ-picoline (Figs. 22 and 23).

*3.2.2.2. The Coats–Redfern method.* The decomposition mechanism for the first step of the processes studied was evaluated from TG curves using the Coats–Redfern, the following equation was used:

$$\ln\left[\frac{g(\alpha)}{T^2}\right] = \ln\left[\frac{AR}{\beta E}\left(1 - \frac{2RT}{E}\right)\right] - \frac{E}{RT} \quad (9)$$

The kinetic parameters were evaluated from the linear plots of the left-hand side of the above equation against $1/T$ for the non-isotermal decomposition at $6^\circ$ min$^{-1}$. The values for the activation energies are

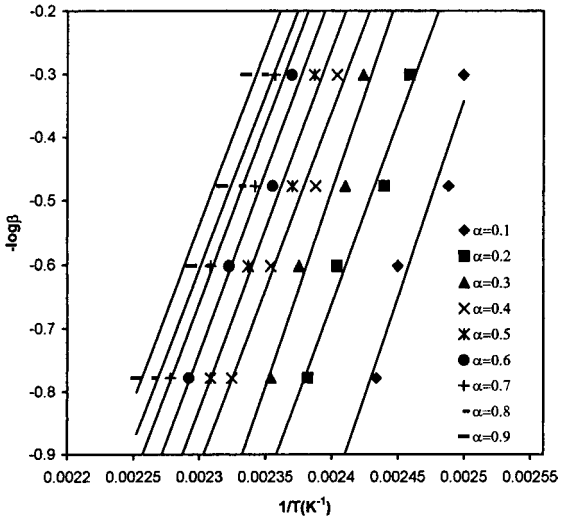


Fig. 23. Isoconversional plots for the non-isothermal decomposition of [Pd(az)Cl(γ-pic)].

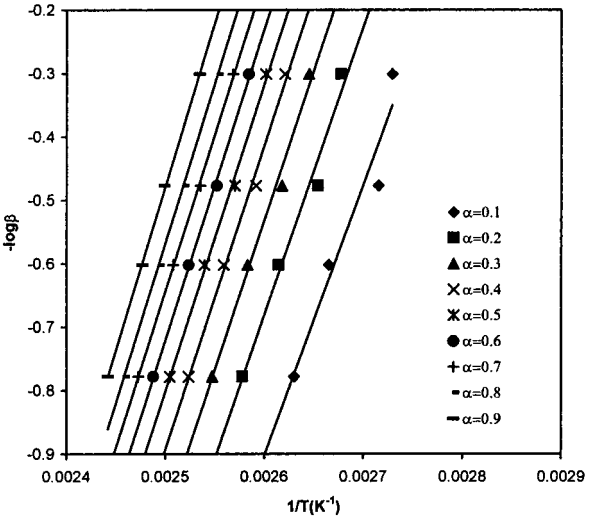


Fig. 25. Isoconversional plots for the non-isothermal decomposition of [Pd(az)I(py)].

Table 4
Apparent activation energies (kJ $mol^{-1}$) calculated for the non-isothermal decomposition using the Coats–Redfern method

| Models | [Pd(az)Cl(py)] | [Pd(az)Br(py)] | [Pd(az)I(py)] | [Pd(az)Cl(α-pic)] | [Pd(az)Cl(γ-pic)] |
|---|---|---|---|---|---|
| $R_2$ | 89 ± 1 | 102 ± 1 | 98 ± 2 | 95 ± 1 | 114 ± 2 |
| $R_3$ | 95 ± 1 | 108 ± 2 | 104 ± 2 | 99 ± 2 | 120 ± 2 |
| $D_1$ | 158 ± 3 | 182 ± 4 | 174 ± 3 | 172 ± 3 | 206 ± 4 |
| $D_2$ | 175 ± 3 | 200 ± 5 | 192 ± 4 | 187 ± 4 | 225 ± 5 |
| $D_3$ | 196 ± 5 | 222 ± 4 | 214 ± 4 | 205 ± 5 | 248 ± 5 |
| $F_1$ | 106 ± 2 | 119 ± 4 | 116 ± 2 | 109 ± 2 | 132 ± 3 |
| $F_2$ | 67 ± 1 | 67 ± 1 | 69 ± 1 | 55 ± 1 | 69 ± 1 |
| $A_{1.5}$ | 69 ± 1 | 77 ± 1 | 75 ± 1 | 71 ± 1 | 86 ± 1 |
| $A_2$ | 50 ± 1 | 56 ± 1 | 55 ± 1 | 51 ± 1 | 63 ± 1 |
| $A_3$ | 31 ± 1 | 35 ± 1 | 34 ± 1 | 32 ± 1 | 39 ± 1 |

shown in Table 4. The best agreement with the results obtained from the isoconversional method is for $F_1$ and $R_n$ kinetic models. The activation energies found for the complexes [Pd(az)Cl(γ-pic)] and [Pd(az)I(py)] by the $A_{1.5}$ mechanism are similar to that calculated by the isoconversional method.

## 4. Conclusions

The results presented above show that the thermal stability of the complexes [Pd(az)ClL] (L = py, α-picoline, γ-picoline) follows the order [Pd(az)Cl(α-picoline)] < [Pd(az)Cl(py)] < [Pd(az)Cl (γ-picoline)], while for the halo-complexes [Pd(az)X(py)] (X = Cl, Br, I) the sequence followed is [Pd(az)I(py)] < [Pd(az)Cl(py)] < [Pd(az)Br(py)]. The activation energies obtained by isothermal and non-isothermal methods are comparable. The kinetic models that best fit the experimental data are $R_n$ and $A_{1.5}$ for isothermal study while for non-isothermal data the most probable mechanisms are $R_n$ and $F_1$.

## References

[1] M.I. Bruce, Angew Chem. Int. Ed. Engl. 16 (1977) 73.
[2] I. Omae, Chem. Rev. 79 (1979) 287.
[3] A. Bahsoun, J. Dehand, M. Pfeffer, M. Zinsius, S.E. Bauaoud, G. Le Borgne, J. Chem. Soc., Dalton Trans. (1979) 547.
[4] A.C. Cope, R.W. Siekman, J. Am. Chem. Soc. 87 (1965) 3273.
[5] B. Crociani, T. Boschi, R. Pietropaolo, U. Belluco, J. Chem. Soc. (A) (1975) 531.
[6] G. Sánchez, I. Solano, M.D. Santana, G. García, J. Gálvez, G. López, Thermochim. Acta 211 (1992) 163.
[7] G. Sánchez, J. García, J. Pérez, G. García, G. López, Thermochim. Acta 307 (1997) 127.
[8] G. Sánchez, J. García, J. Pérez, G. García, G. López, G. Víllora, Thermochim. Acta 293 (1997) 153.
[9] L. Tusek-Bozic, M. Curic, P. Traldi, Inorg. Chim. Acta 254 (1997) 49.
[10] M.I. Bruce, M.J. Liddell, G.N. Pain, Inorg. Synth. 26 (1989) 175.
[11] J.H. Sharp, G.W. Brindley, B.N.N. Achar, J. Am. Ceram. Soc. 49 (1966) 379.
[12] T. Ozawa, Bull. Chem. Soc. Jpn. (1965) 1881.
[13] A.W. Coats, P.J. Redfern, Nature 201 (1964) 68.
[14] C.D. Doyle, J. Appl. Polym. Sci. 6 (1962) 639.
[15] J.H. Flynn, L.A. Wall, Polym. Lett. 4 (1966) 191.